Research Square

Preprints are preliminary reports that have not undergone peer review.
They should not be considered conclusive, used to inform clinical practice,
or referenced by the media as validated information.

Optimizing the process parameters for selective laser-melted Inconel 718

Hemanandan P
Vellore Institute of Technology University
Jeeva P A
pajeeva@vit.ac.in

Vellore Institute of Technology University

Research Article

Keywords: Selective laser melting, grey regression analysis, optimization, Inconel 718

Posted Date: March 4th, 2026

DOI: https://doi.org/10.21203/rs.3.rs-8973888/v1

License: This work is licensed under a Creative Commons Attribution 4.0 International License.
Read Full License

Additional Declarations: No competing interests reported.

Optimizing the process parameters for selective laser-melted Inconel 718

Abstract

Additive manufacturing plays a major role in the latest generation of manufacturing. Selective Laser Melting is the most widely used process in the industry. The study investigates the optimization of process parameter with the Taguchi and Grey relational analysis. The L_9 Taguchi factorial design is utilized with four control variables at three levels. Tensile strength, Hardness and Surface texture have been investigated. When applying Grey relational analysis for multi objective optimization, the optimized parameters are 300 W of laser power, 1000 mm/s of Scan speed, 110 µm of Hatch distance and 30 µm of layer thickness and based on the responses from grades, the level of parameter influence is identified.

Keywords: Selective laser melting, grey regression analysis, optimization, Inconel 718.

1.Introduction

Inconel 718 is a nickel-iron-based alloy, with other elements like chromium, columbium, niobium, molybdenum, etc. It shows excellent corrosion resistance, long fatigue life, high creep strength, and high strength at both room temperature and elevated temperatures [1]. It has good weldability too [2]. It is appropriate to utilize Inconel 718 in high-temperature applications up to 700 °C [3]. In addition to having excellent high-temperature corrosion resistance, IN718 has remarkable tensile and impact resistance also [4]. Due to the excellent strength at elevated temperature, it is widely used in many engineering applications like rotary component of aircraft engines, steam turbine components, gas turbine components, nuclear reactors etc. [5],[6]. The varied properties of alloy 718 can be attributed to its numerous phases, just as those of other alloys. Superalloys possess a highly complicated microstructure. The alloy's behaviour is altered by the presence of several scattered intermetallic and other phases, which vary in composition, shape, and location. The primary phase of alloy 718 is the gamma -phase - Face Centered Cubic (FCC) solid solution, which is composed of several secondary phases like gamma', gamma'', delta phase, Laves phase, Carbides, Topologically Close Packed (TCP) phases and other phases [7] – [9]. Consequently, it is evident that alloy 718's remarkable mechanical properties are the result of the crucial strengthening phase known as gamma'' [10]. The major characteristics of the alloy which are controlled at this phase are tensile, fatigue, and creep [11]. Due to the high hardness and low thermal conductivity, it is very difficult to manufacture IN718 via conventional methods [1]. From the above-mentioned factors in addition to the complexity in shape raise to the usage of Additive Manufacturing (AM) of Inconel 718 [12].

According to ASTM standard, Additive Manufacturing can be defined as "the process of adding materials to create objects" layer by layer [13]. AM can be classified into 7 categories [14]. Laser Powder Bed Fusion (LPBF) is the most suitable technique for the manufacturing of metal parts. It is suitable for small batch production of precise parts [15]. This process is also known as Selective Laser Melting (SLM), Laser Beam Melting (LBM) or Direct Metal Laser Sintering (DMLS). SLM is a cyclical process where a metallic powder bed is partially melted by a laser source, and then a coater applies a fresh layer of powder on top, which melts in the next cycle. Every layer is a slice of the CAD model, and the areas that are going to melt represent the final

component geometry [16]. Some of the advantages of SLM process can be stated as dimensional accuracy, maximum utilization of the powder and freedom of design [17]. Similarly, the disadvantages are porosity, rough surface and formation of residual stress [18]. The process parameters like laser power, scan speed, hatch space and layer thickness play a major role in the porosity and surface finish of the produced part [19]. Various post processing techniques like chemical, mechanical and laser-based process are applied to the additive manufactured parts for the improvement of mechanical and surface properties [20].

2.Materials and Methods

2.1 Machine

In this study EOS M290 machine was used to fabricate the samples made from Inconel 718 powder. The 3D printer is equipped with Yb-fiber laser with the maximum power of 400W and the scanning speed up to 7.0 m/s. This machine has the capability to focus the laser about 100µm. The build volume is 250 x 250 x 325 mm. The print space was protected from environment by supplying the inert argon gas.

2.2 Material

The Inconel 718 powder is gas atomized with the size of the particle ranging from 20 µm to 40 µm. The chemical composition is shown in the Table 1.

Table 1. Elemental composition of Inconel 718.

Element	Ni	Cr	Fe	Nb	Mo	Al	Mn	Si	C	Ti
Wt. %	52.53	20.19	Bal	4.85	3.1	0.5	0.055	0.041	0.025	0.001

2.3 Experiments

The parameters considered were Laser power, scan velocity, hatch space and Layer thickness as these majorly affects the mechanical behavior of the product that decides the suitability of the product for a particular application. This study used Taguchi's L_9 orthogonal array with four parameters and three levels and presented in the

Table *2*.

Table 2. Levels of the parameters (L_9).

Parameter	**Symbol**	**Unit**	**Levels**		
			L1	**L2**	**L3**
Laser Power	LP	W	270	285	300
Scan Speed	SS	mm/s	920	960	1000
Hatch Spacing	HS	µm	80	110	140

Layer Thickness	LT	µm	30	60	90

Two types of Near Net Shape (NNS) specimens were printed. For tensile analysis, the NNS specimens were printed with dog bone shape of dimensions as per ASTM E8 sub size and for microstructure analysis, the NNS specimens of 10mm x 10mm x 5mm were printed. The specimens were printed on the base plate and they were separated using Wire EDM process. For each experimental run, three specimens were prepared and tested and the average values were considered for the analysis.

2.4 Responses

Tensile tests were carried out with the hydraulic Universal Testing machine, Tufan - 400 of capacity 40 kN equipped with displacement and load sensors. Rockwell Hardness was measured by Rockwell testing machine TSM - D0, manufactured by Indian Technologies. Keyence Digital Microscope VHX 7000 N was used to measure the Surface roughness.

2.5 Grey Relational Analysis

Grey Relational Analysis was incorporated to determine the optimal process parameters for selective laser melting process of Inconel 718. It starts with linear normalization of responses as a fraction less than 1 and the expression used as follows [21].

For the responses higher the better, $$z_{i,j} = \frac{y_{i,j} - (min.\, y_{i,j}, i = 1, 2, 3 \cdots n)}{(max.\, y_{i,j}, i = 1, 2, 3 \cdots n - (min.\, y_{i,j}, i = 1, 2, 3 \cdots n))}$$

For the responses lower the better, $$z_{i,j} = \frac{(max.\, y_{i,j}, i = 1, 2, 3 \cdots n) - y_{i,j}}{(max.\, y_{i,j}, i = 1, 2, 3 \cdots n - (min.\, y_{i,j}, i = 1, 2, 3 \cdots n))}$$

Where $y_{i,j}$ is response and $z_{i,j}$ is the normalized response. This step is followed by determining Grey Relational Coefficient (GRC), γ from the following expression,

$$\gamma(z_o, z_{i,j}) = \frac{\Delta_{min.} + \zeta \Delta_{max.}}{\Delta_{oj}(k) + \Delta_{max.}}$$

Where, ζ represents the distinguishing coefficient, in the range of $0 \leq \zeta \leq 1$, Almost in all literatures adopted ζ=0.5 for obtaining the balanced sensitivity of deviation sequence.

$$\Delta_{o,j} = \left| Z_0(k) - Z_{i,j} \right|$$
$$\Delta_{min} = \text{min.} \left| Z_0(k) - Z_{i,j} \right|$$
$$\Delta_{max} = \text{max.} \left| Z_0(k) - Z_{i,j} \right|$$

And finally, the grade was determined by $(z_o, z_{i,j}) = \sum_{k=1}^{n} B_k\, \gamma\,(z_o,\, z_{i,j}) = 1$ while B_k is the assigned weighting factors of the responses.

3. Result and Discussion

3.1 Mechanical Properties

The materials behavior under tensile load is accessed by the tensile test [22]. Figure 1 shows the variations in the tensile strengths of the printed specimens. The specimen 3 registered low tensile strength about 904.1N/mm^2 over others. That may be due to the low volumetric energy density, since, low power at high scanning speed with high hatch distance and high layer thickness results in insufficient energy and time for melting. This results in lack of fusion and ultimately the specimen has low density and high porosity [23]. All other samples except 3 showed negligible variations in the tensile strengths.

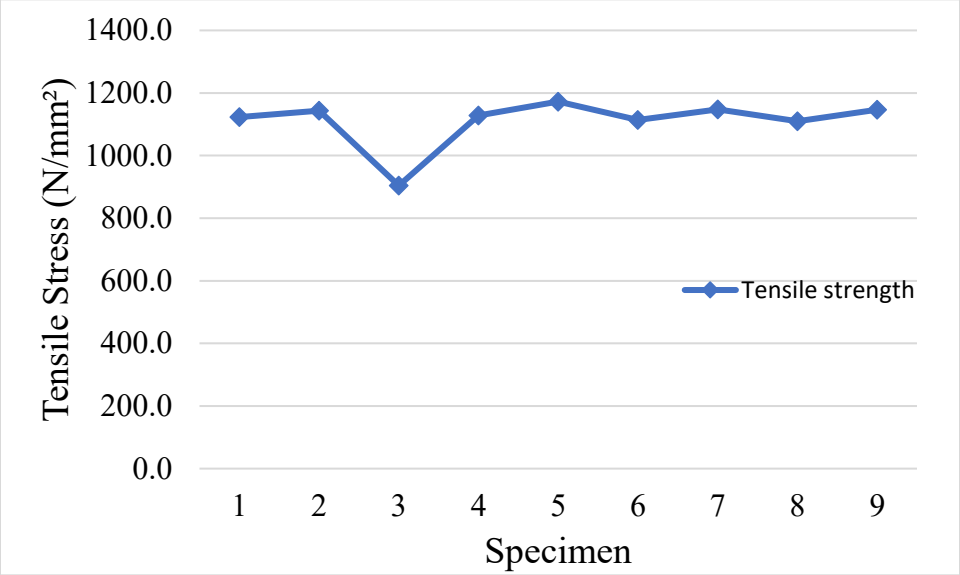


Figure 1. Tensile stress

Figure 2 shows the average value of Rockwell hardness registered by the specimens. Similarly in tensile strength, the variation in the hardness is negligible except 8th one. It showed slightly lesser hardness about 18.5 RC at high laser power and layer thickness. The specimen 8 shows the low rock well hardness. The main reason for the reduced hardness is due to high layer thickness which causes the lack of melting of the powder particles [24].

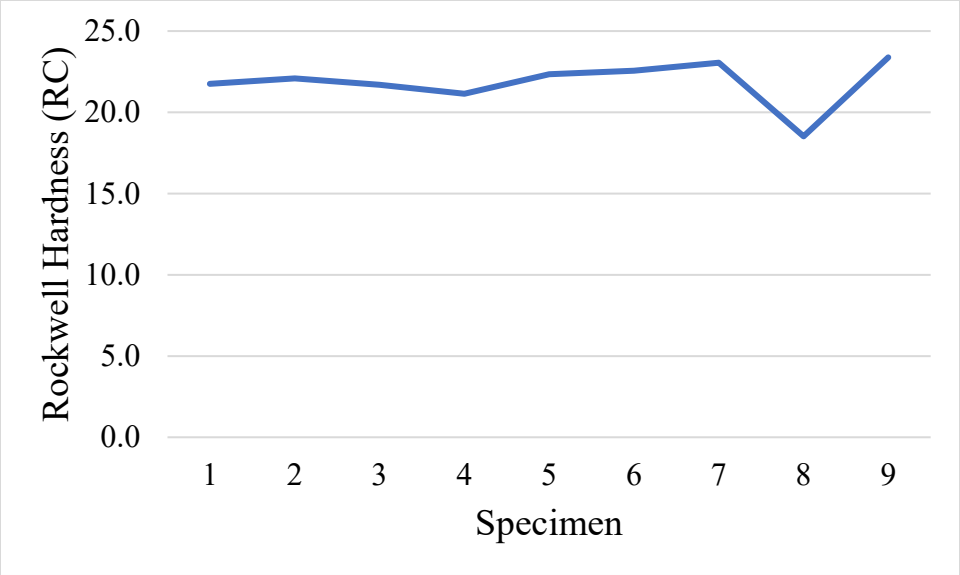


Figure 2. Rockwell hardness

The average values of the roughness measured on each specimen was presented in Figure 3. It shows the considerable variation in the roughness. The sample 4 shows less surface roughness about 0.9 microns and Sample 3 shows the highest roughness of 2.3microns was recorded by the specimen 8.

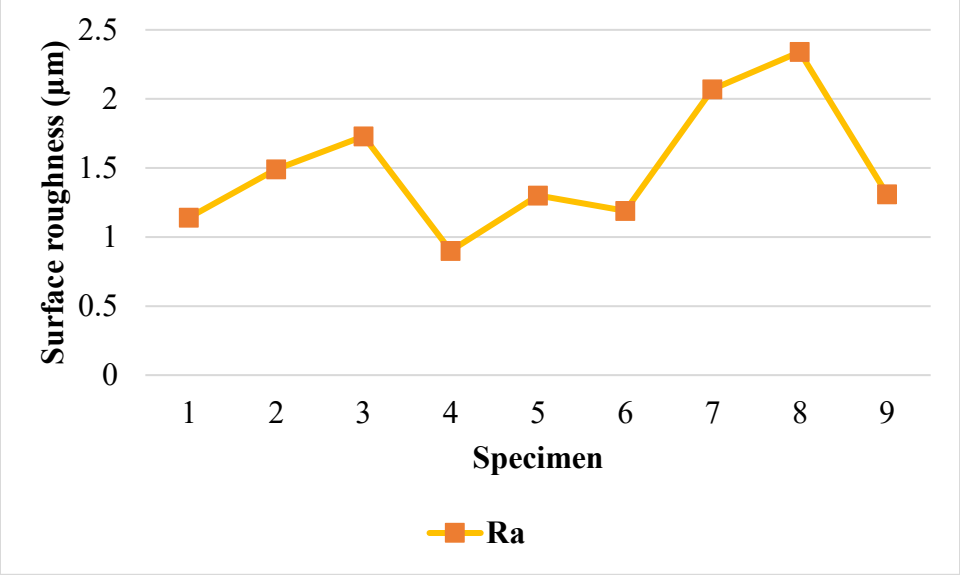


Figure 3. Surface roughness

The surface texture of the specimens captured by the digital microscope is given in Figure 4 below.

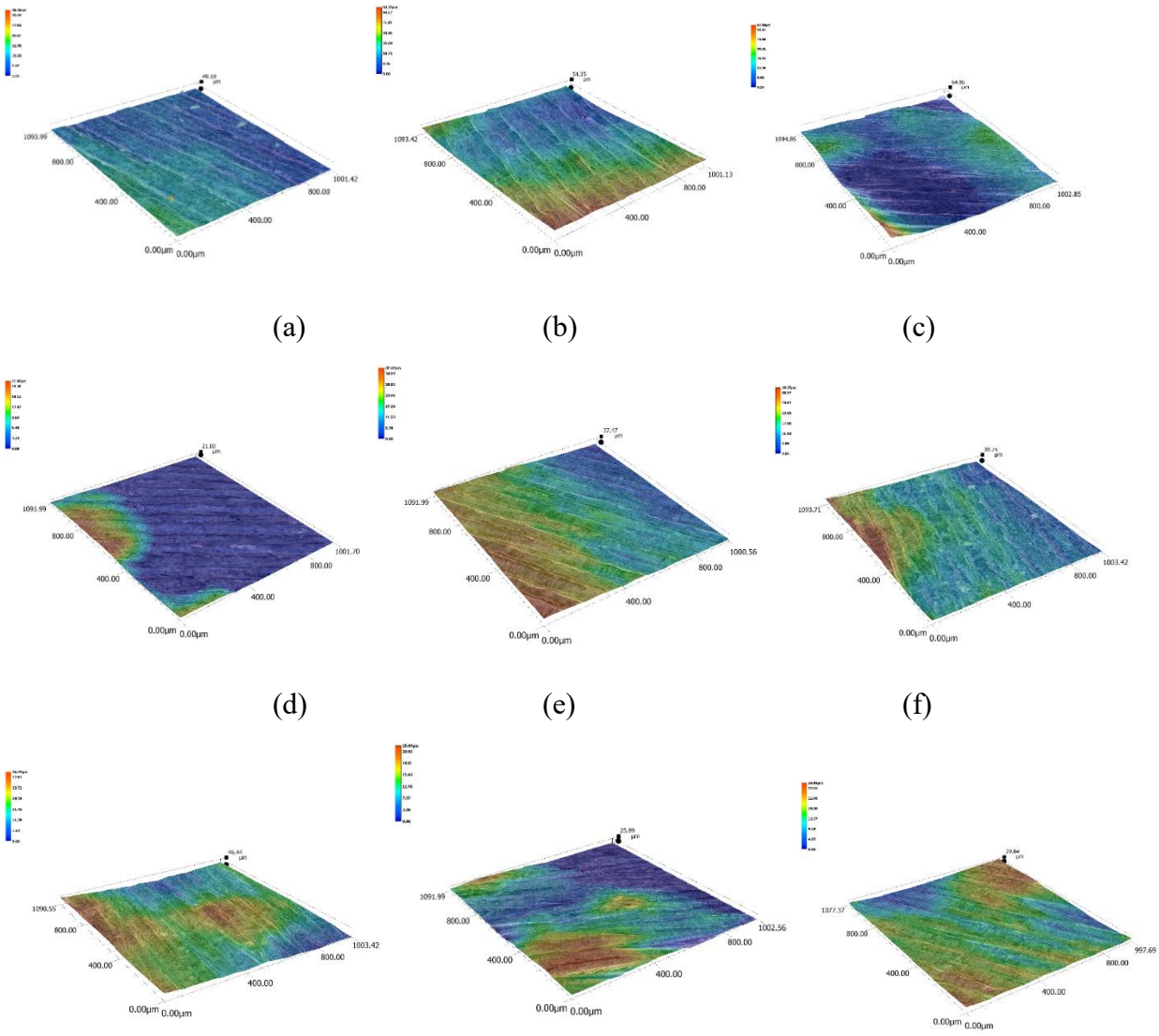


Figure 4. 3D surface texture of the as-built Inconel 718 specimen.

3.2 Weighted Grey relational analysis

GRA was proved as one of the best optimization techniques for experimental studies in determining the parameters for optimum output [25]-[28]. Hence, GRA study was applied to find the best combination of parameters for highest tensile strength, and hardness and lowest surface roughness. As mentioned in the grey relational analysis part in material and methods, the normalized values of responses were found for each experimental run and then grey relational coefficients were found. Finally, grey relational grade was found and presented below in

Table *3*.

Table 3. Grey Relational Coefficients and grades for respective experiments

L9	Grey Relational Coefficients			Grey Relational Coefficients Grades	Rank
	Tensile Strength	Hardness	Surface Roughness		
1	0.7321	0.7500	0.6000	6.265	6
2	0.8243	0.5496	0.6515	6.171	7
3	0.3333	0.4645	0.5912	4.177	8
4	0.7501	1.0000	0.5203	6.760	3
5	1.0000	0.0000	0.7003	7.141	2
6	0.6972	0.7129	0.0000	6.510	4
7	0.8446	0.3810	0.8836	6.495	5
8	0.6795	0.3333	0.3333	4.126	9
9	**0.8361**	**0.6372**	**1.0000**	**7.531**	**1**

Table 4 represents the grades for the responses obtained by averaging the grades of responses corresponding to levels in the experimental design. Based on the concept ‘higher the good’, it is obvious that level 2 of laser power, level 1 of scan speed, level 2 of hatch speed and level 1 of layer thickness.

Table 4. Response table for grade

Parameters	level 1	level 2	level 3	Max-min
Laser Power	5.5375	**6.80358**	6.051	1.26603474
Scan Speed	**6.5065**	5.81285	6.073	0.693656279
Hatch Spacing	5.6335	**6.82065**	5.938	1.187110668
Layer Thickness	**6.9789**	6.39182	5.021	1.957737079

4. Conclusion

The Inconel 718 samples were printed on the base plate and were analyzed for their mechanical properties and the optimum process parameters were found by grey relational analysis. The tensile strength of the specimens was slightly varying and is considerable. The sample with printed with lesser power and higher scan speed, hatch distance and layer thickness showed less tensile strength as the parameter setting leads to improper melting of In718 powder. The highest strength registered under less layer thickness and hatch distance. The sample produced with

higher laser power with low layer thickness registered good hardness about 23.4 RC. Even at higher power, the low layer thick reduces the hardness. The higher power and the low layer thick reduce the Surface roughness greatly. The lower surface roughness was recorded at higher layer thickness and scanning speed. GRA was used to identify the optimum process parameters and the corresponding responses. Layer thickness is highly influencing parameter followed by hatch space, laser power and scan speed.

Funding information

The authors declare that there is no funding to be acknowledged.

Data availability statement

The data will be made available upon reasonable request.

Reference

[1] Hosseini E and Popovich V.A (2019) A review of mechanical properties of additively manufactured Inconel 718. Additive Manufacturing 30: 100877.

[2] Sonar T, Balasubramanian V, Malarvizhi S, Venkateswaran T, Sivakumar D (2021) An overview on welding of Inconel 718 alloy—Effect of welding processes on microstructural evolution and mechanical properties of joints. Mater. Charact 174: 110997

[3] Qi H, Azer M, Ritter A (2009) Studies of standard heat treatment effects on microstructure and mechanical properties of laser net shape manufactured Inconel 718". Metall. Mater. Trans. A 40: 2410–2422.

[4] Ravichander B.B, Mamidi K, Rajendran V, Farhang B, Ganesh Ram A, Hanumantha M, Moghaddam N.S, Amerinatanzi A (2022) Experimental investigation of laser scan strategy on the microstructure and properties of Inconel 718 parts fabricated by laser powder bed fusion. Mater. Charact. 186.

[5] Periane S, Duchosal A, Vaudreuil S, Chibane H, Morandeau A, Cormier J, Leroy R. (2019) Machining influence on the fatigue resistance of Inconel 718 fabricated by selective laser melting (SLM). Procedia Struct. Integr. 19: 415–422.

[6] Liu Z, Kim H, Liu W, Cong W, Jiang Q, Zhang H (2019) Influence of energy density on macro/microstructures and mechanical properties of as-deposited Inconel 718 parts fabricated by laser engineered net shaping. J. Manuf. Process. 42: 96–105

[7] Geddes B, H. Leon and X. Huang. "Superalloys: alloying and performance." 2010, Materials Park, OH: ASM International

[8] Xu Z, C.J. Hyde, C Tuck, and A.T. Clare. (2018) Creep behaviour of Inconel 718 processed by laser powder bed fusion. Journal of Materials Processing Technology 256:13-24

[9] Parimi L.L, G.A. Ravi, D. Clark, and M.M. Attallah. (2014) Microstructural and texture development in direct laser fabricated IN718". Materials Characterization 89: 102-111.

[10] Xu Z, L Cao, Q Zhu, C Guo, X Li, X Hu, and Z Yu. (2020) Creep property of Inconel 718 superalloy produced by selective laser melting compared to forging. Materials Science and Engineering: A.794: 139947

[11] Fournier D and A Pineau. (1977) Low cycle fatigue behavior of Inconel 718 at 298 K and 823 K. Metallurgical Transactions A. 8(7): 1095-1105.
[12] Ptacek L, Nauka o Materi´alu II, 1st ed.; CERM: Brno, Czech Republic, 1999; ISBN 80-7204-130-4
[13] ISO / ASTM52900-15, Standard Terminology for Additive Manufacturing – General Principles - Terminology, ASTM International, West Conshohocken, PA, 2015, www.astm.org.
[14] ASTM S. Standard terminology for additive manufacturing technologies. 2013. F2792-12a
[15] W E Frazier. (2014) Metal additive manufacturing: a review. J. Mater. Eng. Perform. 23: 1917–1928
[16] L Hitzler, M Merkel, W Hall, A Ochsner. (2018) A review of metal fabricated with laser- and powder-bed based additive manufacturing techniques: process, nomenclature, materials, achievable properties, and its utilization in the medical sector. Adv. Eng. Mater. 20: 1–28.
[17] Bartolomeu F, Fonseca J, Peixinho N, Alves N, Gasik M, Silva FS, Miranda G (2019) Predicting the output dimensions, porosity and elastic modulus of additive manufactured bio material structures targeting orthopedic implants. J Mech Behav Biomed Mater 99: 104–117.
[18] T Mishurova, S Cabeza, T Thiede, N Nadammal, A Kromm, M Klaus, C Genzel, C Haberland, and G Bruno (2018) The influence of the support structure on residual stress and distortion in SLM Inconel 718 parts. Metal. Mater. Trans. A. 49: 3038–3046.
[19] Krol M and Tanski T. (2016) Surface Quality Research for Selective Laser Melting of Ti-6al-4v Alloy. Arch. Metall. Mater. 61(3): 1291-1296.
[20] Lee J Y, Nagalingam A P, Yeo S H (2021) A Review on the State-Of-The-Art of Surface Finishing Processes and Related ISO/ASTM Standards for Metal Additive Manufactured Components. Virtual Phys. Prototyp. 16(1): 68–96.
[21] Moqdad Juber Dakhil1, Abdulraheem Khadim AbidAli1, Zainab Al-Khafaji (2026) Optimization of selective laser melting parameters of Ti6Al4V alloys lattice structures utilizing Taguchi method and grey relational analysis. Biomedical Engineering Communications 5(3): 16.
[22] Agarwal Venkesh, J., Samidha, A., Sagar, K., Omkar: (2021) The role of mechanical testing in additive manufacturing: a review. Mater. Sci. Eng. Appl. 1(2): 21–31.
[23] Mohammadamin Bakhtiarian, Hamid Omidvar, Amirhossein Mashhuriazar, Zainuddin Sajuri, C. Hakan Gur (2024) The effects of SLM process parameters on the relative density and hardness of austenitic stainless steel 316L. Journal of Materials Research and Technology. 29: 1616-1629.
[24] Hardik Nadiyadi, Hiren Gajera, Rajnikant Bidajwala, Kumar Abhisek, and Komal Dave (2021) Effects of powder bed fusion process parameters on hardness for Inconel 718. Materials Today: Proceedings. 38(5): 2275-2280.
[25] Akgün M, and Kara F (2021) Analysis and optimization of cutting tool coating effects on surface roughness and cutting forces on turning of AA 6061 alloy. Adv. Mater. Sci. Eng. 1–12.

[26] Thankachan T, Prakash K.S, Malini R, Ramu S, Sundararaj P, Rajandran S, Rammasamy D, Jothi S (2019) Prediction of surface roughness and material removal rate in wire electrical discharge machining on aluminum-based alloys/composites using Taguchi coupled grey relational analysis and artificial neural Networks. Appl. Surf. Sci. 472: 22–35.

[27] Pek¸sen H, and Kalyon A. (2021) Optimization and measurement of flank wear and surface roughness via Taguchi based grey relational analysis. Mater. Manuf. Process" 36: 1865–1874.

[28] Ozlu B. (2022) Evaluation of energy consumption, cutting force, surface roughness and vibration in machining toolox 44 steel using Taguchi based gray relational analysis. Surf. Rev. Lett. 29: 1–17.